

Balanced interactions of calcineurin with AKAP79 regulate Ca²⁺–calcineurin–NFAT signaling

Huiming Li^{1,2,8}, Matthew D Pink^{3,4,8}, Jonathan G Murphy^{3,4}, Alexander Stein^{5,6}, Mark L Dell'Acqua^{3,4} & Patrick G Hogan^{1,7}

In hippocampal neurons, the scaffold protein AKAP79 recruits the phosphatase calcineurin to L-type Ca²⁺ channels and couples Ca²⁺ influx to activation of calcineurin and of its substrate, the transcription factor NFAT. Here we show that an IAIIT anchoring site in human AKAP79 binds the same surface of calcineurin as the PxIxIT recognition peptide of NFAT, albeit more strongly. A modest decrease in calcineurin–AKAP affinity due to an altered anchoring sequence is compatible with NFAT activation, whereas a further decrease impairs activation. Counterintuitively, increasing calcineurin–AKAP affinity increases recruitment of calcineurin to the scaffold but impairs NFAT activation; this is probably due to both slower release of active calcineurin from the scaffold and sequestration of active calcineurin by ‘decoy’ AKAP sites. We propose that calcineurin–AKAP79 scaffolding promotes NFAT signaling by balancing strong recruitment of calcineurin with its efficient release to communicate with NFAT.

Enzyme-scaffold interactions have a critical role in directing intracellular signaling. Scaffolded complexes have been described in multiple signaling pathways and serve as platforms for signal integration and propagation by localizing enzymes in the vicinity of their substrates and regulatory proteins^{1–3}. A notable example is the A-kinase anchoring protein AKAP79, which juxtaposes the kinase PKA with the phosphatase calcineurin and other proteins and targets them to a variety of locations in the plasma membrane^{4,5}.

The protein serine-threonine phosphatase calcineurin (also known as PP2B) is activated when cytoplasmic Ca²⁺ concentrations are elevated, and it regulates a variety of downstream processes in cells. Calcineurin is important for cardiac development and pathophysiology, for nervous-system development and for some of the plastic changes in neurons that are believed to underlie learning and memory^{6–10}. Among the best-characterized substrates of calcineurin are the NFAT transcription factors, NFAT1–NFAT4. Calcineurin–NFAT signaling has been intensely studied for its role in immune-cell activation and as the target of the immunosuppressive drugs cyclosporin A and FK506 (refs. 11,12). These studies led to the identification of a recognition sequence for calcineurin that is shared by many calcineurin substrates and that was first described as having the consensus sequence PxIxIT¹³. We identified a high-affinity version of the PxIxIT sequence, PVIVIT, by selection from a randomized peptide library¹⁴ and used it to define the structural basis of substrate recognition by calcineurin^{15,16} (see also ref. 17). Calcineurin-recognition sites display considerable natural variation in their

sequences and their affinities for calcineurin^{10,16}. The recognition sites of NFAT proteins (PRIET, PSIRIT and PSIQT) display an intermediate K_d of ~25 μ M for calcineurin, whereas the sequences PQIIS in human TRESK and PVIIVN in yeast Hph1 bind calcineurin with K_d s of 5 μ M and 250 μ M, respectively. The strength of individual calcineurin–substrate interactions is an important parameter for intracellular signaling, and, in particular, increasing the strength of a calcineurin–substrate interaction above that of the wild-type proteins can lead to disordered signaling^{10,14,18–20}.

Like many other signaling enzymes, calcineurin is targeted to specific intracellular locations by interactions with scaffold proteins. The scaffold protein AKAP79 is of particular interest because it balances the opposing effects of calcineurin and PKA on neuronal voltage-gated L-type Ca²⁺ channels²¹ and coordinates the activities of calcineurin, PKA and PKC on a number of other channels and receptors^{22–28}. In rat hippocampal neurons, NFAT signaling is initiated by the local elevation of Ca²⁺ concentration near L-type Ca²⁺ channels^{21,29}. RNA interference (RNAi)-mediated depletion of endogenous AKAP150, the rat ortholog of human AKAP79, eliminates NFAT activation in neurons, which, however, can be rescued by expression of human AKAP79 (ref. 21). A conserved calcineurin-binding site has been mapped in AKAP79 (Fig. 1a), and deletion of this anchoring sequence eliminates the ability of AKAP79 to rescue NFAT activation, despite abundant calcineurin elsewhere in the cytoplasm, emphasizing the local nature of calcineurin–NFAT signaling and the importance of calcineurin scaffolding by AKAP79 in these cells^{21,30}.

¹Immune Disease Institute and Program in Cellular and Molecular Medicine, Children's Hospital, Boston, Massachusetts, USA. ²Department of Pediatrics, Harvard Medical School, Boston, Massachusetts, USA. ³Department of Pharmacology, University of Colorado School of Medicine, Anschutz Medical Campus, Aurora, Colorado, USA. ⁴Program in Neuroscience, University of Colorado School of Medicine, Anschutz Medical Campus, Aurora, Colorado, USA. ⁵Howard Hughes Medical Institute, Harvard Medical School, Boston, Massachusetts, USA. ⁶Department of Cell Biology, Harvard Medical School, Boston, Massachusetts, USA. ⁷La Jolla Institute for Allergy & Immunology, La Jolla, California, USA. ⁸These authors contributed equally to this work. Correspondence should be addressed to P.G.H. (phogan@liai.org) or M.L.D. (Mark.DellAcqua@ucdenver.edu).

Received 21 August 2011; accepted 23 December 2011; published online 19 February 2012; doi:10.1038/nsmb.2238

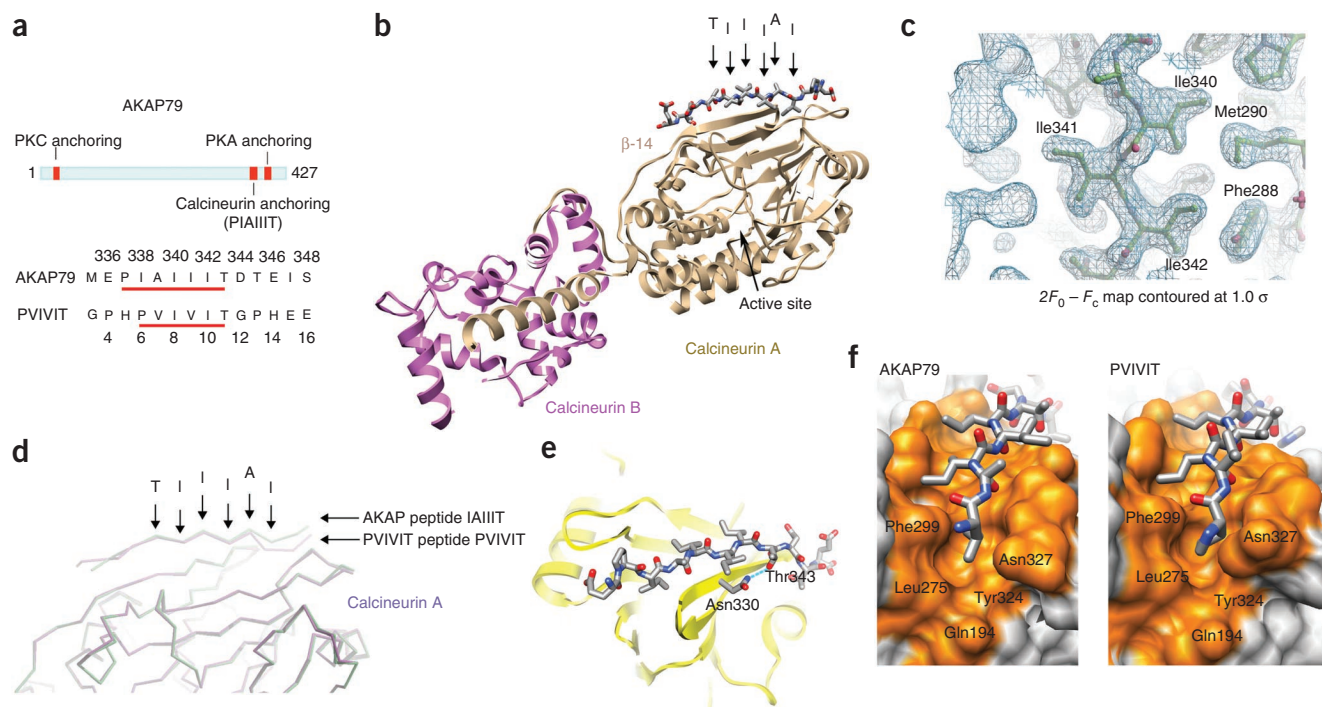


Figure 1 Crystal structure of calcineurin in complex with AKAP79 peptide. **(a)** Location of the PxlXIT-like calcineurin-anchoring site within human AKAP79 protein and sequence comparison to the PVIVIT peptide. The numbering of the residues in AKAP79 and in PVIVIT peptide is shown above and below the sequences, respectively. **(b)** Overall structure of calcineurin A and calcineurin B in complex with AKAP79 peptide. The key residues comprising the core calcineurin-binding motif are indicated. **(c)** A $2F_o - F_c$ map contoured at 1σ showing the electron density surrounding the isoleucine stretch, Ile340–Ile342, of the IAIIT calcineurin-anchoring motif of AKAP79. **(d)** Superposition of the calcineurin–AKAP79 peptide structure onto the previously solved calcineurin–PVIVIT structure. The core calcineurin-binding residues of AKAP79 are labeled as in **b**. **(e)** The hydrogen bond between Thr343 of AKAP79 and Asn330 of CNA recapitulates a critical contact^{13,15} in the calcineurin–PVIVIT structure. **(f)** Side-by-side comparison of the calcineurin–AKAP79 structure (left) and calcineurin–PVIVIT structure (right) viewed from the ‘proline pocket’ defined in the calcineurin–PVIVIT structure. Calcineurin is shown in surface representation with residues in direct contact with the peptides colored orange, and the peptides are displayed in stick representation. The figures were prepared using Chimera³⁸ and Coot³⁹.

To gain further insight into the role of this calcineurin-scaffold interaction in intracellular signaling, we have investigated its structural basis, the affinity and kinetics of calcineurin–AKAP79 binding, and the effects of relatively small perturbations of the interaction on NFAT transcriptional signaling in cells. The crystal structure of a calcineurin–AKAP79 complex shows that calcineurin engages an atypical PxlXIT site in AKAP79. The functional studies lead to three principal conclusions: first, despite the absence of a consensus proline residue, the AKAP79 site binds calcineurin more tightly than any of the recognition peptides identified so far in substrates; second, the site allows rapid dissociation of calcineurin for physiological signaling; and, third, only a rather narrow window of calcineurin–AKAP79 affinities is compatible with normal NFAT signaling. We propose that the atypical PxlXIT site of AKAP79 meets two independent requirements of intracellular signaling, in that it (i) recruits calcineurin efficiently to the vicinity of L-type Ca^{2+} channels for activation by Ca^{2+} entering the cell and yet (ii) allows the disengagement of calcineurin to couple channel activation with downstream signaling events.

RESULTS

Structure of the calcineurin–AKAP79 complex

To define the structural basis for calcineurin binding to AKAP79, we crystallized the complex of calcineurin with an AKAP79 peptide and solved its structure at 2.0-Å resolution (Table 1 and Fig. 1b; PDB 3LL8). Two calcineurin A–calcineurin B (CNA–CNB) heterodimers

and one AKAP peptide are contained in the asymmetric unit. As in the calcineurin–PVIVIT structure¹⁶ that describes consensus calcineurin-substrate recognition, the AKAP79 PIAIIIT peptide is in closer contact with one of the two calcineurin heterodimers in the asymmetric unit.

The electron density in the calcineurin–AKAP complex is well defined throughout the core of the AKAP recognition peptide and the apposed surface of calcineurin (Fig. 1c). The AKAP peptide assumes an extended configuration as a β -strand aligned along β -strand 14 of CNA on a surface distant from the catalytic site (Fig. 1b–d). Seven backbone hydrogen bonds serve to position the peptide strand between AKAP residues Ala339 and Thr345 as part of an extended β sheet.

In the core region of calcineurin–AKAP peptide contact, Ile340 and Ile342 of AKAP make contacts on a nonpolar surface of calcineurin in the trough between β -strand 11 and β -strand 14 (Fig. 1c), and Thr343 forms a hydrogen bond with Asn330 of CNA (Fig. 1e). These contacts are identical to those of the corresponding isoleucine and threonine side chains in the calcineurin–PVIVIT structure. Strikingly, however, Ile338 of AKAP takes the position of Pro6 in the calcineurin–PVIVIT complex (Fig. 1f). The Ile338 side chain is buried in the pocket to approximately the same depth as Pro6 in the calcineurin–PVIVIT complex, resulting in a slight displacement of the backbone at Ile338 away from the calcineurin surface compared to PVIVIT (Fig. 1d). In the N-terminal flanking region of the AKAP peptide, the electron density of Glu336 and Pro337 is poorly defined and does not

Table 1 Data collection and refinement statistics (molecular replacement)

CNA–CNB–AKAP79 complex	
Data collection	
Space group	$P2_12_12_1$
Cell dimensions <i>a</i> , <i>b</i> , <i>c</i> (Å)	86.28, 89.70, 158.91
Resolution (Å)	50.0–2.00 (2.07–2.00) ^a
R_{sym}	7.1 (50.3)
$I / \sigma I$	16.2 (1.9)
Completeness (%)	95.7 (91.5)
Redundancy	3.1 (2.9)
Refinement	
Resolution (Å)	50.0–2.00
No. reflections	75,502
$R_{\text{work}}/R_{\text{free}}$	17.8/22.8
No. atoms	
Protein	8363
Ligand/ion	22
Water	583
<i>B</i> -factors	
Protein	38.6
Ligand/ion	33.4
Water	49.7
R.m.s. deviations	
Bond lengths (Å)	0.017
Bond angles (°)	1.6

^aValues in parentheses are for highest-resolution shell.

contact CNA. The C-terminal flanking region of the AKAP peptide makes van der Waals contacts on the surface of calcineurin, and the hydrogen bond network anchoring the flanking region of the calcineurin–PVIVIT complex is supplanted by Thr343–Asn333 and Asp344–Lys318 contacts. There is no sequence conservation among PxlIT sites from different calcineurin-binding proteins in the segments flanking the core recognition peptide, and the idiosyncratic contacts of AKAP are consistent with the view¹⁶ that PxlIT flanking regions arrange themselves in a low-energy configuration but may not contribute appreciably to $\Delta G_{\text{binding}}$.

Solution studies of the calcineurin–AKAP79 complex

We sought to complement the picture from X-ray crystallography by experimental characterization of calcineurin–AKAP79 binding in solution. Size-exclusion chromatography coupled with multi-angle light scattering (SEC-MALS) showed a shift in migration of the calcineurin heterodimer peak upon formation of a complex with AKAP79_{333–408} and an increase in mass of ~8 kDa, corresponding to a 1:1 complex of calcineurin with AKAP79_{333–408} (Fig. 2a).

The crystal structure offers two possible modes of contact in a 1:1 complex, and in both modes the AKAP79 peptide occupies roughly the same surface of calcineurin (Fig. 2b). The peptide is aligned in each case along β -strand 14 of calcineurin and is stabilized by backbone hydrogen bonds to β strand 14. Contact mode 1 buries 1,332 Å² of surface and makes seven backbone hydrogen bonds, whereas contact mode 2 buries 820 Å² and makes four backbone hydrogen bonds. The two contact modes differ most prominently in whether the Ile338 side chain is in contact with calcineurin (Fig. 2b). In the calcineurin–AKAP peptide structure already described, Ile338 is buried in the ‘proline pocket’ of the PxlIT-binding surface, whereas in the alternative complex it extends away from calcineurin. An I338A

substitution substantially reduced the affinity of the calcineurin–AKAP peptide interaction in a competitive binding assay (Fig. 2c), indicating that Ile338 contributes to calcineurin–AKAP binding, consistent with contact mode 1. Finally, although neither calcineurin–peptide contact in the crystal structure involves Pro337, the substantial energetic contribution of the Pro6 contact in the calcineurin–PVIVIT complex¹⁶ led us to introduce a P337A substitution to rule out alternative modes of binding that bury Pro337. The P337A mutation had no impact on calcineurin–AKAP affinity in the competitive binding assay (Fig. 2c). The combined SEC-MALS and competitive binding data establish that calcineurin binding at the IAIIT site in solution gives a 1:1 complex and support the structural model depicted in Figure 1b,f.

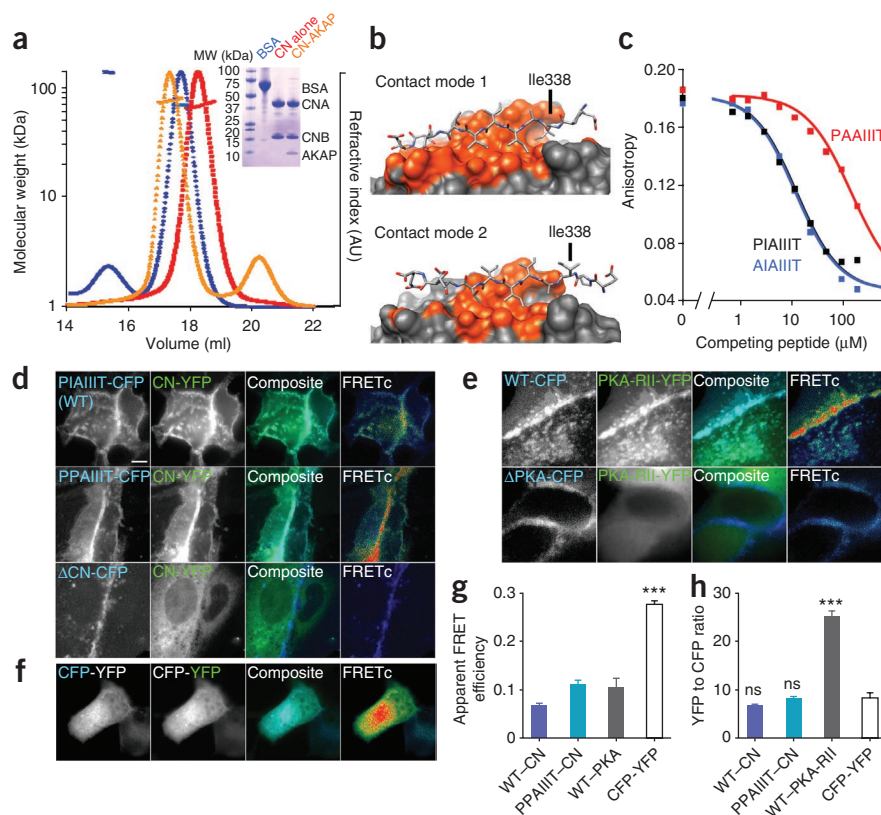
Stoichiometry of the calcineurin–AKAP79 complex in living cells

To determine whether calcineurin and full-length AKAP79 also form a 1:1 complex in living cells, we compared YFP/CFP fluorescence intensity ratios measured in MDCK cells expressing calcineurin–YFP and AKAP79–CFP to the ratios measured in cells expressing a reference CFP–YFP protein covalently linking CFP to YFP or in cells expressing RII–YFP and AKAP79–CFP (Fig. 2d–h). As shown in our previous work^{21,31,32}, coexpression of calcineurin–YFP (Fig. 2d) or PKA–RII–YFP (Fig. 2e) with wild-type AKAP79–CFP resulted in colocalization of the YFP-labeled proteins with AKAP79 at the plasma membrane and in fluorescence resonance energy transfer (FRET) between CFP and YFP. Both the plasma membrane colocalization of CFP and YFP and the FRET signals were eliminated by deletion of the respective anchoring sites in AKAP79 (Δ CN, Fig. 2d; Δ PKA, Fig. 2e)²¹. In the cases of calcineurin and RII, we applied a mask to the images in order to determine the YFP/CFP ratio specifically at membrane sites of colocalization and FRET. After correcting CFP fluorescence intensity for the quenching due to FRET, the YFP/CFP ratio of the calcineurin–wild-type AKAP79 pair was 6.6 ± 0.5 , not significantly different from the YFP/CFP ratio of 8.5 ± 1.0 observed for 1:1 linked CFP–YFP (Fig. 2h). Replacing wild-type AKAP79 with the I338P variant discussed below to ensure high binding-site occupancy increased the YFP/CFP ratio only to 8.1 ± 0.6 , still not significantly different from that of linked CFP–YFP. The YFP/CFP ratio of the RII–wild-type AKAP pair (25.2 ± 1.2) was, as expected, significantly greater than that of the 1:1 construct, in fact exceeding the reference value by more than a factor of 2. One explanation for the excess YFP signal is that a minor fraction of RII–YFP is free or in complexes not involving AKAP79–CFP. There is no specific evidence whether or not there is such an excess YFP signal in the calcineurin experiments, but any calcineurin–YFP not complexed with AKAP79–CFP would lead to an overestimate, rather than an underestimate, of calcineurin in the calcineurin–AKAP79 complex. The YFP/CFP ratio measurements are most consistent with the formation of a 1:1 calcineurin–AKAP79 complex and a 2:1 RII–AKAP79 complex in cells and are in agreement with our SEC-MALS data for the calcineurin–AKAP79 complex (Fig. 2a) and the known structure of the RII–AKAP79 complex³³.

Calcineurin binding to and dissociation from the IAIIT site

The IAIIT anchoring site is essential for NFAT signaling in hippocampal neurons because it underlies recruitment of calcineurin to AKAP79 complexes adjacent to the L-type Ca²⁺ channel²¹. Recruitment of calcineurin to AKAP-scaffolded complexes in neurons will depend on the concentration of free calcineurin and on the K_d of the binding interaction. To obtain a direct estimate of calcineurin–AKAP79 K_d , we made quantitative measurements of FRET between an ATTO425–AKAP79_{333–408} donor and rhodamine–calcineurin acceptor

Figure 2 The calcineurin–AKAP79 complex in solution. (a) SEC-MALS analysis of calcineurin alone (red), calcineurin–AKAP complex (orange) and BSA standard (blue). Inset, corresponding SDS-polyacrylamide gel. AU, arbitrary units. (b) Alternative 1:1 complexes based on the two calcineurin molecules in the crystal asymmetric unit. The figures were prepared using Chimera³⁸. (c) Competition of the indicated GST-AKAP79_{333–348} fusion proteins with fluorescent PVIVIT peptide for binding to calcineurin. The estimated K_S are AIAIIIT, 3.7 μM ; PIAIIIT, 3.9 μM ; PAIIIT, 47 μM . Total competitor concentration (not free concentration) is plotted. Data shown are representative of three experiments. (d,e) Images of living MDCK cells showing membrane colocalization (turquoise in composite panels) and corrected CFP donor to YFP acceptor FRET gated to the CFP channel (FRETc; pseudocolor, blue = no FRET to red = high FRET) for the indicated AKAP79-CFP proteins (blue) and calcineurin A–YFP (CN–YFP) (d; green) or PKA–RII–YFP (e; green). Scale bar, 5 μm . (f) CFP, YFP and FRETc images as above for a linked CFP–YFP construct. (g) Measurements of apparent FRET efficiency, used to correct CFP fluorescence intensity for quenching. (h) Corrected YFP/CFP fluorescence intensity ratios for experiments in d–f. Statistical comparisons were by one-way ANOVA with a Bonferroni post-hoc test; *** $P < 0.001$ and $^{ns}P > 0.05$ compared to the linked CFP–YFP standard ($n = 10–41$ cells). Error bars, s.e.m.



(Supplementary Fig. 1a,b). Titration with increasing concentrations of calcineurin yielded a binding curve at room temperature that could be fitted with K_d 0.4 μM (Fig. 3a,b and Supplementary Fig. 1c,d), supporting the K_d estimated independently from kinetic measurements, ~ 0.3 μM (Fig. 3c,d). We conclude that interaction at the IAIIT site can effectively recruit calcineurin in neurons if the free calcineurin concentration is in the high hundreds of nanomolar to low micromolar range.

The rapid dissociation of calcineurin–AKAP79 peptide complex is particularly relevant to the transmission of intracellular signals. Even though AKAP79 and NFAT use the same surface to dock on calcineurin, recruitment of calcineurin to AKAP79 need not be in conflict with productive signaling because of the rapid equilibration

between free calcineurin and AKAP-bound calcineurin. Experiments reported below establish that dissociation at physiological temperature is even more rapid than in the experiment of Figure 3.

Scaffold interaction and calcineurin–NFAT signaling

Knowledge of the calcineurin–AKAP79 structure opens an opportunity to investigate the effect of systematically varying the affinity of this enzyme–scaffold interaction. Building on our earlier studies of the calcineurin–PVIVIT structure and the rules that connect changes in the sequence of calcineurin–recognition sites in substrates to variations in affinity¹⁶, we designed a small panel of AKAP79 anchoring peptides whose affinities for calcineurin span a wide range. The peptides contained the replacements I338P, T343A or both. Wild-type and variant AKAP proteins are referred to by 7-mer sequences to facilitate comparison with variant sequences of the variations introduced—for instance, a peptide containing the wild-type anchoring sequence is designated PIAIIIT, even though Pro337 is not part of the contact interface defined in the crystal structure. Competitive binding experiments in which these unlabeled AKAP variants, as GST fusion proteins, were used to displace labeled PVIVIT demonstrated that the relative affinities were PPIIIIT > PIAIIIT > PPIIIA > PIAIIIA,

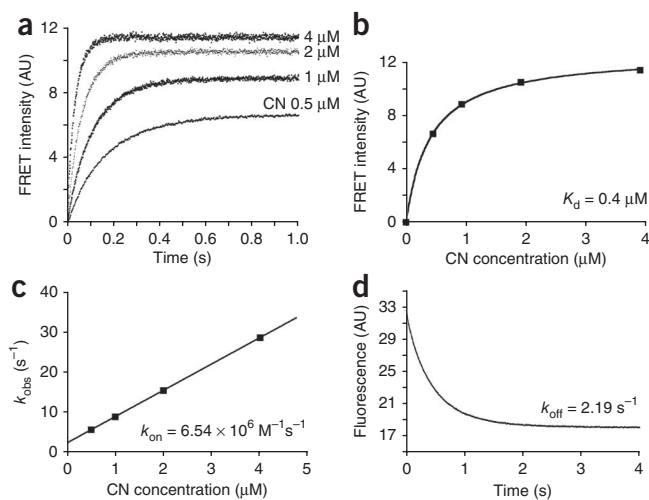
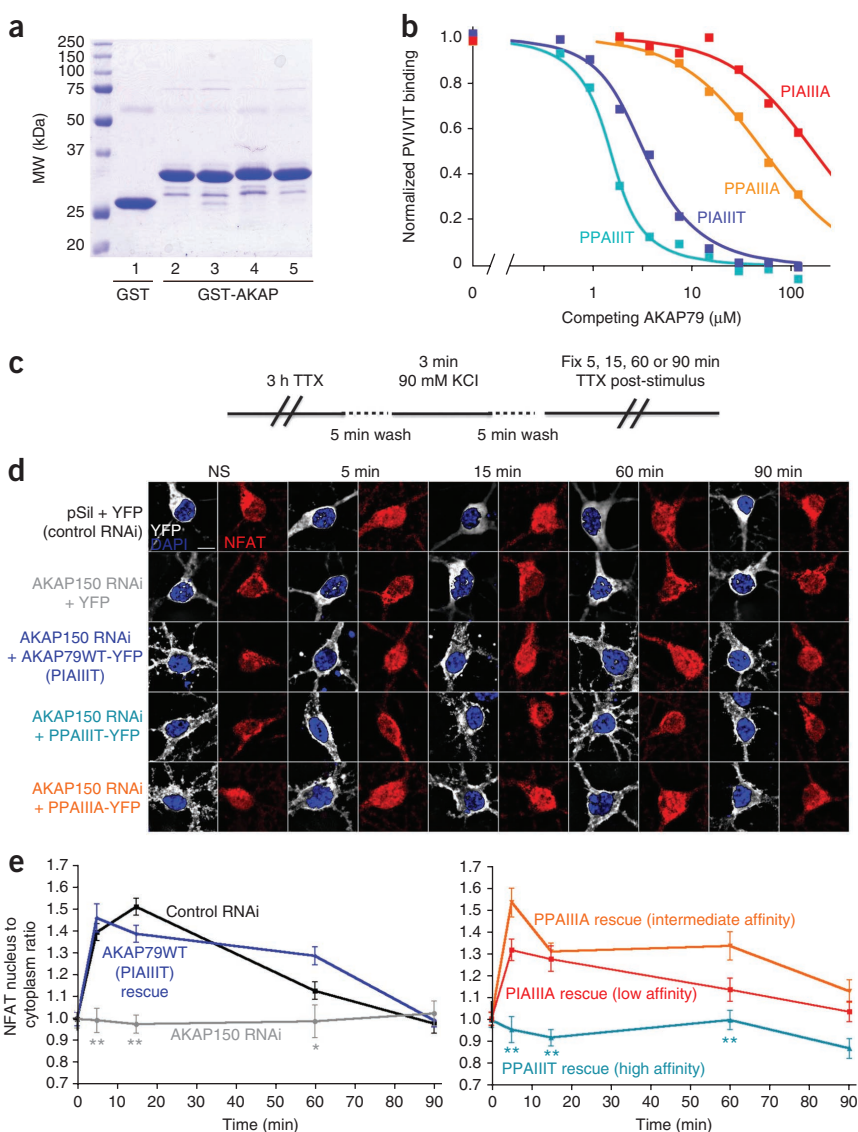


Figure 3 Equilibrium and kinetic measurements of calcineurin binding to AKAP79. (a) Calcineurin (CN) binding to AKAP79_{333–408} was monitored by stopped-flow FRET measurements. The observed time course of binding at 22 $^{\circ}\text{C}$ is shown for four calcineurin concentrations. (b) A plot of plateau FRET intensities against calcineurin concentrations. (c) The association rate constant k_{on} estimated from the data in a based on a model of reversible binding to a single class of sites. (d) Dissociation of the calcineurin–AKAP79_{333–408} complex at 22 $^{\circ}\text{C}$. In this AKAP79_{333–408} protein, the RII α -anchoring site was replaced by the AKAP-*in silico* (AKAP-IS) sequence^{33,40}. Data shown are representative of two experiments. AU, arbitrary units.

Figure 4 A high-affinity AKAP79 variant, PPAIIIT, does not support NFAT nuclear translocation in hippocampal neurons.

(a) Recombinant GST, GST-tagged wild-type AKAP79₃₃₃₋₄₀₈ (PIAIIIT, lane 2), and the variants PIAIIIA, PPAIIIA and PPAIIIT (lanes 3–5) were analyzed by SDS-PAGE and staining with Coomassie Brilliant Blue. (b) K_d s estimated in a competitive binding assay are PPAIIIT, 0.08 μ M; wild type, 0.36 μ M; PPAIIIA, 12 μ M; and PIAIIIA, 39 μ M. Total competitor concentration (not free concentration) is plotted. Data shown are representative of three experiments. (c) KCl stimulus protocol previously shown to activate L-type Ca^{2+} -channel signaling through calcineurin in hippocampal neurons^{21,29}. (d) Summed intensity projection images of neuronal cell bodies and proximal dendrites in non-stimulated (NS) cultures and in cultures fixed at the indicated times after KCl stimulation. Transfection with control RNAi plasmid (pSil), AKAP150 RNAi plasmid and RNAi-resistant expression plasmids is indicated. The paired images show YFP or AKAP-YFP (white), DAPI-stained nuclei (blue) and endogenous NFAT (red). Scale bar, 10 μ m. (e) Time course of NFAT nuclear import after KCl stimulation, from experiments as in d, quantified as nucleus-to-cytoplasm mean fluorescence intensity ratios²¹. Each point represents $n = 12$ –25 neurons, and in each case the data have been normalized to the value for non-stimulated cultures ($t = 0$ min). Statistical comparisons were by one-way ANOVA with a Bonferroni post-hoc test, * $P < 0.05$ and ** $P < 0.01$ compared to AKAP79WT rescue. Error bars, s.e.m.



covering more than a 100-fold range in K_d (Fig. 4a,b). Notably, the PPAIIIT variant, in which Ile338 was substituted with proline, bound about four-fold more strongly to calcineurin than wild-type AKAP79.

To explore the biological effect of varying the affinity of calcineurin-scaffold interactions, we expressed full-length AKAP79 proteins with either the wild-type PIAIIIT anchoring sequence or one of the variant sequences PPAIIIT, PPAIIIA and PIAIIIA in rat hippocampal neurons. The neurons were depolarized by elevating KCl concentration, using a stimulus protocol that activates L-type Ca^{2+} -channel signaling through calcineurin and triggers NFAT nuclear translocation and NFAT-dependent gene expression^{21,29}. Endogenous NFAT3 (also known as NFATc4) was localized immunocytochemically. As shown previously, RNAi-resistant wild-type human AKAP79 rescued NFAT nuclear translocation in neurons after depletion of endogenous AKAP150 by RNAi (Fig. 4c–e). AKAP79 bearing the lower-affinity sequences also rescued NFAT nuclear translocation, AKAP79 with PPAIIIA (intermediate affinity) as efficiently as wild-type AKAP79, and AKAP79 with PIAIIIA (lowest affinity) somewhat less efficiently (Fig. 4d,e). Previous work has shown that AKAP79 lacking the calcineurin-anchoring site does not rescue calcineurin-NFAT signaling²¹. Unexpectedly, AKAP79 bearing the higher-affinity sequence PPAIIIT was also completely unable to rescue signaling (Fig. 4d,e).

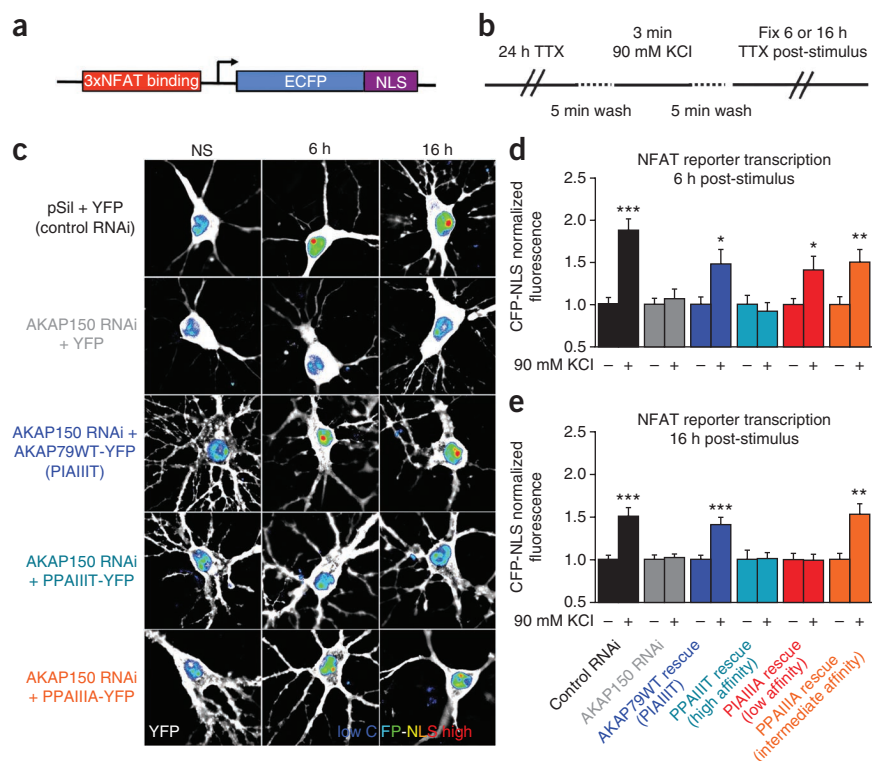
The differences in NFAT nuclear localization have practical consequences for NFAT-dependent transcription (Fig. 5). Endogenous

AKAP150 in rat hippocampal neurons was depleted by RNAi as for the nuclear import experiments, the cells were reconstituted with human AKAP79 and its variants, and NFAT-dependent transcription was monitored as expression of a 3xNFAT-ECFP reporter. Wild-type AKAP79 and AKAP79 with PPAIIIA (intermediate affinity) were equivalent in rescuing transcription (Fig. 5c–e). Consistent with its effect on NFAT nuclear translocation, the low-affinity PIAIIIA AKAP79 was partially functional, as evidenced by rescue of NFAT transcription only at an early time (Fig. 5d) but not at a later time after stimulation (Fig. 5e). PPAIIIT was again completely unable to rescue NFAT signaling (Fig. 5c–e).

Altered calcineurin interactions with the PPAIIIT site

Among the possible reasons for the failure of PPAIIIT to support signaling was unavailability of calcineurin to bind NFAT after calcineurin activation at the scaffold complex associated with the L-type Ca^{2+} channel. We compared dissociation of calcineurin from its complexes with wild-type AKAP79₃₃₃₋₄₀₈ (PIAIIIT) and with the PPAIIIT variant in stopped-flow FRET experiments at room temperature and at 36 °C (Fig. 6a,b and Supplementary Fig. 2). Preformed calcineurin-AKAP79 complex was mixed with an excess of unlabeled PVIVIT

Figure 5 The high-affinity AKAP79 variant PPAIIIT does not couple Ca^{2+} influx to NFAT-dependent transcription in hippocampal neurons. **(a)** Diagram of the 3xNFAT-AP1-CFP-NLS transcriptional reporter construct used for single-cell imaging of NFAT-dependent transcription. **(b)** Modified KCl stimulation protocol used to assay L-type Ca^{2+} -channel activation of NFAT-dependent reporter-gene transcription in hippocampal neurons. **(c)** Summed intensity projection images of neuronal cell bodies and proximal dendrites in non-stimulated (NS) cultures and in cultures fixed at the indicated times after KCl stimulation for neurons transfected with the 3xNFAT-AP1-CFP-NLS reporter along with the indicated RNAi, YFP and AKAP79-YFP constructs as in **Figure 4d**. YFP fluorescence is in white and nuclear-localized CFP fluorescence is in pseudocolor with a relative scale from blue (low intensity) to red (high intensity). **(d,e)** Quantification of CFP reporter-gene expression 6 h **(d)** or 16 h **(e)** after KCl stimulation (+) from experiments as in **c**, normalized to the non-stimulated condition (-). * $P < 0.05$, ** $P < 0.01$ and *** $P < 0.001$ by Student's *t*-test compared to the respective non-stimulated condition ($n = 11$ –50 neurons). Error bars, s.e.m.



peptide to prevent rebinding of calcineurin to AKAP79, and complex dissociation was monitored as the decrease in the FRET signal. The dissociation of calcineurin from wild-type AKAP79 was rapid at both temperatures, with the mean dissociation rate at 36 °C, 9.96 s⁻¹ (range 8.84–11.84 s⁻¹, $n = 4$), corresponding to a half-time of ~70 ms (**Fig. 6a**). The implication is that calcineurin can rapidly expose its NFAT-binding surface even if that surface is initially engaged in a physiological complex with wild-type AKAP79. Dissociation of the higher-affinity calcineurin–PPAIIIT AKAP79 complex was appreciably slower, with

mean dissociation rate 4.24 s⁻¹ (range 3.90–4.55 s⁻¹, $n = 4$) and corresponding half-time ~163 ms (**Fig. 6b**), consistent with a modest reduction in availability of the docking surface to interact with NFAT after calcineurin activation in cells.

We undertook a second line of experiments to gain insight into the anchoring of calcineurin by AKAP79 in living cells. We examined the dynamics, and more specifically the mobile fraction, of calcineurin-YFP in rat hippocampal neuron dendritic spines using fluorescence

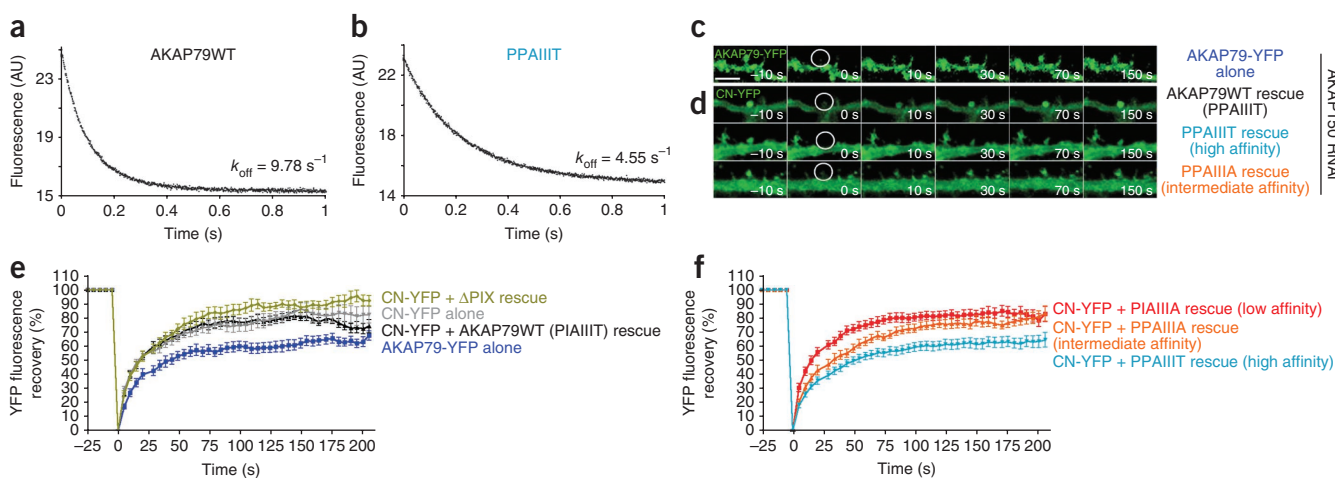


Figure 6 The high-affinity AKAP79 PPAIIIT variant decreases the rate of calcineurin dissociation *in vitro* and reduces the mobility of calcineurin in dendritic spines. **(a,b)** Dissociation of calcineurin from wild-type AKAP79_{333–408} **(a)** and its I338P variant **(b)** at 36 °C. AU, arbitrary units. **(c)** Time-lapse images of wild-type AKAP79-YFP fluorescence recovery in single dendritic spines of rat hippocampal neurons in culture at the indicated times after photobleaching. A pre-bleach image ($t = -10$ s) is shown for comparison. **(d)** YFP fluorescence recovery in neurons cotransfected with calcineurin A-YFP (CN-YFP) and CFP-tagged wild-type AKAP79 (AKAP79WT) or CFP-tagged AKAP79 variants (PPAIIIT, PPAIIIA) as indicated. CFP fluorescence is not shown. **(e,f)** Percent YFP fluorescence recovery plotted against time for the FRAP experiments illustrated in **c** and **d** and for similar experiments with the other AKAP79 variants PPAIIIA and ΔPIX (deletion of PPAIIIT). In the experiment with CN-YFP alone, transfection with the RNAi plasmid was omitted. Maximal percent recovery (mobile fraction) values stated in the text were calculated from the curves in **e** and **f** by fitting a single exponential function. Statistical *P* values stated in the text were determined by one-way ANOVA with a Bonferroni post-hoc test ($n = 10$ –28 neurons). Error bars **(e,f)**, s.e.m.

recovery after photobleaching (FRAP). Endogenous AKAP150 was depleted by RNAi and replaced with wild-type or mutant AKAP79. Coexpression of calcineurin-YFP with the Δ PIX variant (deletion of PIAIIT), which cannot bind calcineurin, led to a significant increase in the mobile fraction of calcineurin ($89.5 \pm 0.7\%$, $P < 0.001$) compared to rescue with wild-type AKAP79 ($77.5 \pm 0.6\%$) or the intermediate affinity PPAIIIA variant ($77.1 \pm 0.8\%$) (Fig. 6c–f). Coexpression with the low-affinity PIAIIIA variant also gave a modest, but still significant, increase in mobile fraction ($81.3 \pm 0.6\%$, $P < 0.01$) consistent with reduced anchoring of calcineurin to this variant (Fig. 6f). In contrast, AKAP with the high-affinity site PPAIIIT decreased the mobile fraction of calcineurin ($61.6 \pm 0.7\%$, $P < 0.001$ compared to wild type) (Fig. 6d,f) to a level that was very similar to that of the less mobile AKAP79 itself ($61.8 \pm 0.6\%$) (Fig. 6c,e). The variant AKAP79 proteins were all expressed at the same levels across experiments, as was calcineurin-YFP, and there was no change in the mobile fraction of AKAP79 with any variant tested (Supplementary Fig. 3). These results indicate that calcineurin-AKAP binding contributes perceptibly to the immobilization of calcineurin in dendritic spines, and that an increase in calcineurin-AKAP affinity that blocks NFAT signaling is reflected in an increase in calcineurin anchored by AKAP in the spine. Note that the calcineurin immobilization detected in cells extends to a much longer time scale than calcineurin-AKAP79 dissociation *in vitro* and thus probes a different aspect of calcineurin interaction with PPAIIIT, as discussed below.

DISCUSSION

Our studies provide strong evidence that the IAIIT recognition peptide makes a principal contribution to calcineurin-AKAP79 anchoring *in vitro* and in cells. In fact, the sequence IAIIT shows the highest affinity so far observed for a natural calcineurin-recognition site, with a measured K_d less than $1 \mu\text{M}$. Competitive binding assays with the PAAIIT, PIAIIIA and AIAIIT variant peptides and larger AKAP fragments document the importance of the Ile338 and Thr343 contacts for calcineurin-AKAP79 binding in solution, and support the structural model presented here as the basis for calcineurin-AKAP79 binding. Comparison of calcineurin binding to the 14-mer peptide and to AKAP79_{333–408} (Figs. 2c and 4b) suggests a small additional energetic contribution from AKAP79 residues outside the IAIIT site, but the essential interaction is with the core anchoring site. The evidence that calcineurin forms a 1:1 complex with the primary anchoring site does not rule out a 2:1 complex of calcineurin with AKAP79 (ref. 34) if the complex is stabilized by other interactions.

The involvement of AKAP79 scaffolding in calcineurin-NFAT signaling in hippocampal neurons poses competing requirements: calcineurin must use its PxlIT-interacting surface to bind AKAP79 adjacent to L-type Ca^{2+} channels, but the same surface must be

available to recognize NFAT. The level of calcineurin in brain is high, $\sim 1\%$ of soluble protein³⁵, translating to a total calcineurin concentration in the cell cytoplasm of $\sim 10 \mu\text{M}$. Allowing for calcineurin bound to partner proteins, a plausible free calcineurin concentration in neurons is in the high hundreds of nanomolar to low micromolar range, in which case the majority of AKAP79 sites in neuronal cells will be occupied by calcineurin at any given time. Nevertheless, the rapid dissociation of the calcineurin-AKAP79 peptide complex *in vitro* indicates that the docking surface on calcineurin is in principle available for efficient interaction with NFAT and other cellular substrates.

Only AKAP79 proteins with calcineurin-scaffold affinities in a relatively narrow window, $0.4\text{--}12 \mu\text{M}$, were as effective as wild-type AKAP79 in supporting calcineurin-NFAT signaling. The impaired signaling seen with low-affinity AKAP79 (PIAIIIA) and the loss of signaling with AKAP lacking the calcineurin-anchoring site are readily explained by a failure to recruit sufficient calcineurin to scaffold complexes associated with L-type Ca^{2+} channels (Fig. 7). Although the intermediate-affinity AKAP79 (PPAIIIA) supports NFAT signaling, it may not be biologically interchangeable with wild-type AKAP79: nuclear import of NFAT is a relatively insensitive measure, which requires an experimental design with a fairly strong Ca^{2+} signal, and the same strong Ca^{2+} signal was used for transcriptional assays in order to drive measurable transcription with a 3-min stimulus. The window for NFAT signaling may well be narrower at low levels of physiological stimulation.

Unexpectedly, despite its modestly increased affinity for calcineurin, AKAP79 with the PPAIIIT sequence impaired NFAT signaling rather than further promoting it. A partial explanation is that the higher affinity decreased the release of active calcineurin from AKAP79 into the cytoplasm (Fig. 7). Similarly, the PRIEIT > PRIEIA substitution in NFAT1 causes only a ten-fold shift in K_d but eliminates calcineurin-NFAT signaling in T cells¹³. Indeed, simplified mathematical models predict a very sharp dependence of NFAT activation on calcineurin activity³⁶. Nevertheless, the fact that the two- to four-fold shifts in calcineurin-AKAP79 affinity and dissociation rate produced by the I338P substitution are associated with a complete loss of calcineurin-NFAT signaling suggests that a second process may be involved.

The FRAP experiments provide a strong indication of the nature of this second process. An increased fraction of calcineurin is immobilized by binding to AKAP79 with the PPAIIIT anchoring site, and this measure may in fact understate the sequestration of calcineurin by altered AKAP, because more than half of the AKAP79 in the

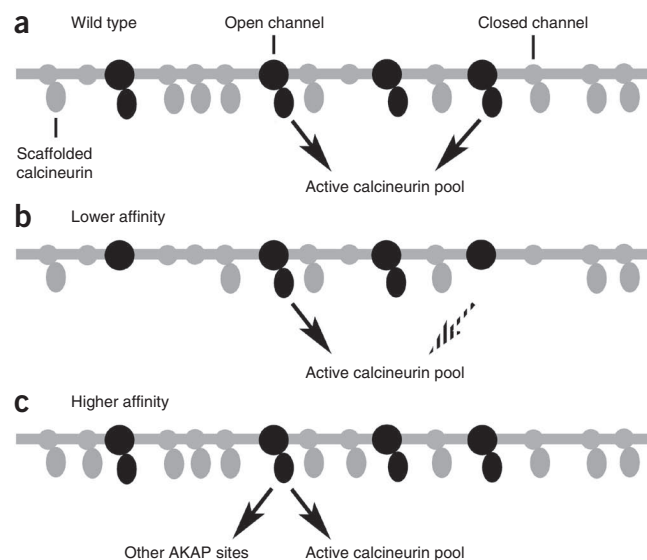


Figure 7 Model explaining the effects of altered calcineurin-AKAP79 anchoring interactions. (a) With wild-type AKAP79, most calcineurin-anchoring sites at the L-type Ca^{2+} channel are occupied. Both inactive and active calcineurin are continually released from the scaffold sites and replaced, so that any activated calcineurin rapidly becomes available to interact with NFAT. Release of inactive calcineurin is not depicted. (b) Low-affinity anchoring sites are partially occupied. Calcineurin release from the scaffold sites is efficient, but only occupied sites contribute active calcineurin at any instant in time, and thus the rate of release of active calcineurin is reduced compared to wild-type AKAP79. (c) High-affinity anchoring sites are fully occupied. The rate of release of calcineurin is somewhat reduced and, at any given time, a larger fraction of the active calcineurin is in complex with other AKAP79 scaffold sites than in the case of wild-type AKAP79.

dendritic spines is itself mobile on the time scale examined. Thus we consider it likely that the decreased release of active calcineurin into the cytoplasm is compounded by calcineurin binding to 'decoy' AKAP79 sites at the L-type Ca^{2+} channel and elsewhere, which act in competition with the NFAT substrate (Fig. 7). A parallel situation has been observed in yeast, where the engineered high-affinity substrate Crz1(PVIVIT) diverts calcineurin from other substrates whose dephosphorylation is necessary for the response to alkaline pH¹⁸.

Our FRAP experiments indicate that a fraction of calcineurin in hippocampal neurons is immobilized by AKAP79 on a considerably longer time scale than that required for dissociation of calcineurin-AKAP complexes *in vitro*. These results imply that at least some calcineurin-AKAP complexes are stabilized by additional interactions in cells, such as interactions through a subsidiary calcineurin-binding site in AKAP (ref. 34), interactions with other proteins known to associate with AKAP79, or tethering of CNB to the cell membrane through its myristoyl modification. If calcineurin is held by additional interactions, the correlate in cells of the complete dissociation of the calcineurin-AKAP79 complex observed *in vitro* might be a 'breathing' of the calcineurin-IAIIIT contact that exposes the PxIXIT-binding surface of calcineurin but does not result in full dissociation of the assembled protein complex.

In summary, the conserved IAIIIT anchoring sequence of AKAP79 provides a high-affinity binding site to recruit calcineurin to the vicinity of the L-type Ca^{2+} channel, where calcineurin can be activated by Ca^{2+} influx, while at the same time preserving a dynamic interaction that permits sufficient unbinding to allow active calcineurin to recognize NFAT. We speculate that the binding affinity has been finely tuned during evolution by these competing requirements, perhaps leaving the interaction poised at the single affinity that maintains calcineurin-substrate communication across the range of physiological signal strengths. The more general conclusion is that a third element, the precise strength of docking interactions, must be included in the description of intracellular signaling networks, in addition to the connectivity of the signaling networks determined by scaffold proteins and the modulatory interactions that can occur within individual scaffold complexes^{1-3,37}. Our experiments illustrate the precise tailoring of calcineurin-scaffold docking affinity to the requirements of signaling in hippocampal neurons and suggest that a similar matching of affinity to signaling may occur in other pathways built upon transient protein-protein interactions.

METHODS

Methods and any associated references are available in the online version of the paper at <http://www.nature.com/nsmb/>.

Accession codes. The crystallographic data have been deposited in the Protein Data Bank under accession code 3LL8.

Note: Supplementary information is available on the Nature Structural & Molecular Biology website.

ACKNOWLEDGMENTS

We are grateful to the Department of Neurobiology, Harvard Medical School, for use of its spectrofluorometer, and to S. Lehrer, Boston Biomedical Research Institute, for access to the stopped-flow instrument. Diffraction data were collected at the Advanced Photon Source on Northeastern Collaborative Access Team beamline 24-ID-C, which is supported by award RR15-301 from the National Center for Research Resources at the US National Institutes of Health. Use of the Advanced Photon Source, an Office of Science User Facility operated for the US Department of Energy (DOE) Office of Science by Argonne National Laboratory, was supported by the US DOE under Contract No. DE-AC02-06CH11357. We thank A. Sorkin, University of Pittsburgh, for providing the tandem YFP-CFP construct. The work was supported by US National Institutes of Health grants

AI40127 (to A. Rao and P.G.H.), MH080291 (to M.L.D.) and AI090428 (to H.L.). M.D.P. was supported in part by T32NS007083 and by an American Heart Association Predoctoral Fellowship from the Pacific Mountain Affiliate. J.G.M. was supported in part by T32HD041697.

AUTHOR CONTRIBUTIONS

H.L. prepared the recombinant calcineurin and AKAP79 proteins, carried out the X-ray crystallography, developed the FRET assay for calcineurin-AKAP interaction and performed equilibrium binding measurements. H.L. and P.G.H. analyzed data from these experiments. H.L. and A.S. carried out SEC-MALS measurements. H.L. and P.G.H. performed and analyzed the stopped-flow kinetic experiments. M.D.P., J.G.M. and M.L.D. carried out and analyzed the FRET and YFP/CFP ratio measurements in MDCK cells. M.D.P. and M.L.D. carried out and analyzed the NFAT localization and FRAP experiments with hippocampal neurons. J.G.M. and M.L.D. carried out and analyzed the transcriptional reporter experiments with hippocampal neurons. P.G.H. and H.L. drafted the manuscript, with significant contributions from M.L.D., M.D.P. and J.G.M.

COMPETING FINANCIAL INTERESTS

The authors declare no competing financial interests.

Published online at <http://www.nature.com/nsmb/>.

Reprints and permissions information is available online at <http://www.nature.com/reprints/index.html>.

- Zeke, A., Lukacs, M., Lim, W.A. & Remenyi, A. Scaffolds: interaction platforms for cellular signalling circuits. *Trends Cell Biol.* **19**, 364–374 (2009).
- Scott, J.D. & Pawson, T. Cell signaling in space and time: where proteins come together and when they're apart. *Science* **326**, 1220–1224 (2009).
- Good, M.C., Zalatan, J.G. & Lim, W.A. Scaffold proteins: hubs for controlling the flow of cellular information. *Science* **332**, 680–686 (2011).
- Coghlan, V.M. *et al.* Association of protein kinase A and protein phosphatase 2B with a common anchoring protein. *Science* **267**, 108–111 (1995).
- Logue, J.S. & Scott, J.D. Organizing signal transduction through A-kinase anchoring proteins (AKAPs). *FEBS J.* **277**, 4370–4375 (2010).
- Hogan, P.G., Chen, L., Nardone, J. & Rao, A. Transcriptional regulation by calcium, calcineurin, and NFAT. *Genes Dev.* **17**, 2205–2232 (2003).
- Molkentin, J.D. & Dorn, G.W. II. Cytoplasmic signaling pathways that regulate cardiac hypertrophy. *Annu. Rev. Physiol.* **63**, 391–426 (2001).
- Heineke, J. & Molkentin, J.D. Regulation of cardiac hypertrophy by intracellular signalling pathways. *Nat. Rev. Mol. Cell Biol.* **7**, 589–600 (2006).
- Groth, R.D., Dunbar, R.L. & Mermelstein, P.G. Calcineurin regulation of neuronal plasticity. *Biochem. Biophys. Res. Commun.* **311**, 1159–1171 (2003).
- Li, H., Rao, A. & Hogan, P.G. Interaction of calcineurin with substrates and targeting proteins. *Trends Cell Biol.* **21**, 91–103 (2011).
- Feske, S., Okamura, H., Hogan, P.G. & Rao, A. Ca^{2+} /calcineurin signalling in cells of the immune system. *Biochem. Biophys. Res. Commun.* **311**, 1117–1132 (2003).
- Macian, F. NFAT proteins: key regulators of T-cell development and function. *Nat. Rev. Immunol.* **5**, 472–484 (2005).
- Aramburu, J. *et al.* Selective inhibition of NFAT activation by a peptide spanning the calcineurin targeting site of NFAT. *Mol. Cell* **1**, 627–637 (1998).
- Aramburu, J. *et al.* Affinity-driven peptide selection of an NFAT inhibitor more selective than cyclosporin A. *Science* **285**, 2129–2133 (1999).
- Li, H., Rao, A. & Hogan, P.G. Structural delineation of the calcineurin-NFAT interaction and its parallels to PP1 targeting interactions. *J. Mol. Biol.* **342**, 1659–1674 (2004).
- Li, H., Zhang, L., Rao, A., Harrison, S.C. & Hogan, P.G. Structure of calcineurin in complex with PVIVIT peptide: portrait of a low-affinity signalling interaction. *J. Mol. Biol.* **369**, 1296–1306 (2007).
- Takeuchi, K., Roehrl, M.H., Sun, Z.Y. & Wagner, G. Structure of the calcineurin-NFAT complex: defining a T cell activation switch using solution NMR and crystal coordinates. *Structure* **15**, 587–597 (2007).
- Roy, J., Li, H., Hogan, P.G. & Cyert, M.S. A conserved docking site modulates substrate affinity for calcineurin, signaling output, and *in vivo* function. *Mol. Cell* **25**, 889–901 (2007).
- Roy, J. & Cyert, M.S. Cracking the phosphatase code: docking interactions determine substrate specificity. *Sci. Signal.* **2**, re9 (2009).
- Shi, Y. Serine/threonine phosphatases: mechanism through structure. *Cell* **139**, 468–484 (2009).
- Oliveria, S.F., Dell'Acqua, M.L. & Sather, W.A. AKAP79/150 anchoring of calcineurin controls neuronal L-type Ca^{2+} channel activity and nuclear signaling. *Neuron* **55**, 261–275 (2007).
- Dell'Acqua, M.L. *et al.* Regulation of neuronal PKA signaling through AKAP targeting dynamics. *Eur. J. Cell Biol.* **85**, 627–633 (2006).
- Wong, W. & Scott, J.D. AKAP signalling complexes: focal points in space and time. *Nat. Rev. Mol. Cell Biol.* **5**, 959–970 (2004).
- Hoshi, N. *et al.* AKAP150 signaling complex promotes suppression of the M-current by muscarinic agonists. *Nat. Neurosci.* **6**, 564–571 (2003).



25. Hoshi, N., Langeberg, L.K. & Scott, J.D. Distinct enzyme combinations in AKAP signalling complexes permit functional diversity. *Nat. Cell Biol.* **7**, 1066–1073 (2005).
26. Tavalin, S.J. *et al.* Regulation of GluR1 by the A-kinase anchoring protein 79 (AKAP79) signaling complex shares properties with long-term depression. *J. Neurosci.* **22**, 3044–3051 (2002).
27. Liu, G. *et al.* Assembly of a Ca²⁺-dependent BK channel signaling complex by binding to β 2 adrenergic receptor. *EMBO J.* **23**, 2196–2205 (2004).
28. Tunquist, B.J. *et al.* Loss of AKAP150 perturbs distinct neuronal processes in mice. *Proc. Natl. Acad. Sci. USA* **105**, 12557–12562 (2008).
29. Graef, I.A. *et al.* L-type calcium channels and GSK-3 regulate the activity of NF-ATc4 in hippocampal neurons. *Nature* **401**, 703–708 (1999).
30. Dell'Acqua, M.L., Dodge, K.L., Tavalin, S.J. & Scott, J.D. Mapping the protein phosphatase-2B anchoring site on AKAP79. Binding and inhibition of phosphatase activity are mediated by residues 315–360. *J. Biol. Chem.* **277**, 48796–48802 (2002).
31. Oliveria, S.F., Gomez, L.L. & Dell'Acqua, M.L. Imaging kinase–AKAP79–phosphatase scaffold complexes at the plasma membrane in living cells using FRET microscopy. *J. Cell Biol.* **160**, 101–112 (2003).
32. Gorski, J.A., Gomez, L.L., Scott, J.D. & Dell'Acqua, M.L. Association of an A-kinase-anchoring protein signaling scaffold with cadherin adhesion molecules in neurons and epithelial cells. *Mol. Biol. Cell* **16**, 3574–3590 (2005).
33. Gold, M.G. *et al.* Molecular basis of AKAP specificity for PKA regulatory subunits. *Mol. Cell* **24**, 383–395 (2006).
34. Gold, M.G. *et al.* Architecture and dynamics of an A-kinase anchoring protein 79 (AKAP79) signaling complex. *Proc. Natl. Acad. Sci. USA* **108**, 6426–6431 (2011).
35. Stemmer, P. & Klee, C.B. Serine/threonine phosphatases in the nervous system. *Curr. Opin. Neurobiol.* **1**, 53–64 (1991).
36. Salazar, C. & Hofer, T. Allosteric regulation of the transcription factor NFAT1 by multiple phosphorylation sites: a mathematical analysis. *J. Mol. Biol.* **327**, 31–45 (2003).
37. Bashor, C.J., Horwitz, A.A., Peisajovich, S.G. & Lim, W.A. Rewiring cells: synthetic biology as a tool to interrogate the organizational principles of living systems. *Annu. Rev. Biophys.* **39**, 515–537 (2010).
38. Pettersen, E.F. *et al.* UCSF Chimera—a visualization system for exploratory research and analysis. *J. Comput. Chem.* **25**, 1605–1612 (2004).
39. Emsley, P. & Cowtan, K. Coot: model-building tools for molecular graphics. *Acta Crystallogr. D Biol. Crystallogr.* **60**, 2126–2132 (2004).
40. Alto, N.M. *et al.* Bioinformatic design of A-kinase anchoring protein-*in silico*: a potent and selective peptide antagonist of type II protein kinase A anchoring. *Proc. Natl. Acad. Sci. USA* **100**, 4445–4450 (2003).

ONLINE METHODS

Additional methods. Further details about cDNA constructs, protein expression and characterization, structure determination, culture of hippocampal neurons, fluorescence microscopy and data analysis are provided in **Supplementary Methods**.

Crystallization and structure determination. Purified calcineurin–AKAP79 complex, 7 mg/ml in 20 mM TES pH 7.0, 50 mM CaCl₂, 1 mM DTT, was mixed 1:1 with reservoir buffer containing 50 mM TES pH 7.5, 15% PEG 20,000, 100 mM MgSO₄, 2 mM DTT and was incubated as sitting drops at 20 °C. Small, plate-shaped crystals appeared overnight and continued to grow to about 0.4 × 0.15 × 0.05 mm³ in a week. X-ray diffraction data were collected on NE-CAT beamline 24-ID-C at the Advanced Photon Source. Wavelength of data collection, 0.9789 Å; temperature, 105 K. Diffraction data from one single crystal were used. The structure was solved by molecular replacement using the coordinates of a CNA–CNB complex from PDB entry 2P6B as a search model in Phaser⁴¹ and refined to 2.0 Å resolution using CNS⁴². Ramachandran statistics: 96.8% favored, 0.2% outliers.

SEC-MALS. SEC-MALS experiments were performed on a light-scattering system (Wyatt Technology Corp.) comprising a DAWN EOS detector and an Optilab rEX refractive index detector coupled to an ÅKTA Purifier (GE Healthcare) and analyzed using Astra V software (Wyatt Technology).

Calcineurin–AKAP79 competitive binding assays. The ability of GST-AKAP79_{333–408} and GST-AKAP79_{333–348} fusion proteins to compete with fluorescent PVIVIT peptide for binding to calcineurin was measured¹⁵. Competitive displacement data were analyzed with a simple competitive binding model^{43,44} as described in detail in **Supplementary Methods**.

FRET-based stopped-flow binding assays. AKAP79_{333–408} was labeled with ATTO 425 donor (ATTO-TECH), and calcineurin with tetramethylrhodamine acceptor (Invitrogen). FRET-based stopped-flow experiments were performed using a HI-TECH KinetAsyst stopped-flow system (model SF-61SX2; TgK Scientific). Labeled AKAP79 concentration was 100 nM. In dissociation measurements, a preformed complex of labeled AKAP79 and calcineurin was mixed with 100 μM (final concentration) unlabeled PVIVIT peptide. Kinetic data were modeled as single exponential processes, and FRET plateau data were modeled as binding at a single class of sites.

YFP/CFP fluorescence ratio measurements in cells. Living MDCK cells expressing AKAP79–CFP, CNAα–YFP, PKA–RIIα–YFP or linked CFP–YFP as indicated were imaged at room temperature. Three-filter FRET images were captured^{21,31,32}, apparent FRET efficiency (FRETEff) values were calculated as described in **Supplementary Methods**, and the observed YFP/CFP fluorescence intensity ratios were corrected for CFP quenching due to FRET. Calculation of FRETEff depends on the acceptor:donor stoichiometry of the complex (**Supplementary Methods**). For RII, FRETEff and the corrected YFP/CFP ratio were calculated based on the known 2:1 complex. For calcineurin, both 1:1 and 2:1 complexes were considered. Corrected YFP/CFP ratios for calcineurin–AKAP pairs treated as 1:1 complexes (6.6 ± 0.5 for wild-type AKAP79, 8.1 ± 0.6 for the PPAIIIT variant) or treated as 2:1 complexes (6.1 ± 0.4 for wild-type AKAP79, 7.1 ± 0.5 for the PPAIIIT variant) differed only minimally and did not exceed the ratio for the 1:1 CFP–YFP construct. Therefore, in **Figure 2g,h**, only FRETEff values and corrected YFP/CFP ratios for a 1:1 calcineurin–AKAP79 complex are plotted.

Primary culture and transfection of rat hippocampal neurons. Neurons were cultured as described⁴⁵. We have shown that the pSil-ShRNAi AKAP150 vector effectively knocks down AKAP150 expression in hippocampal neurons for 2–12 d post transfection^{21,25,46} and allows its replacement with human AKAP79.

NFAT translocation assays. Cultured hippocampal neurons were incubated in Tyrode's salt solution with 1 μM TTX (Tocris) at 37 °C, 5% CO₂, for 3 h to dampen spontaneous activity and lower basal levels of nuclear NFAT^{21,25,46}. Neurons were stimulated by a 3-min depolarization with isotonic 90 mM KCl Tyrode's solution; then, after 5, 15, 60 or 90 min of further incubation in Tyrode's solution containing 1 μM TTX at 37 °C, 5% CO₂, the cells were fixed, permeabilized and stained for endogenous NFAT3 (also termed NFATc4)⁴⁵. Nuclei were counterstained with DAPI.

NFAT transcriptional reporter assays. Hippocampal cultures were transfected with an NFAT-AP1 reporter plasmid that drives expression of ECFP fused to three copies of the SV40 nuclear localization sequence. TTX (1 μM) was added to the medium for 24 h before stimulation to dampen spontaneous activity and decrease basal CFP expression. After a 3-min depolarization with isotonic 90 mM KCl, cells were further incubated in the presence of 1 μM TTX for 6 or 16 h before fixation, permeabilization and counterstaining of nuclei with propidium iodide.

FRAP microscopy. A micro-point tunable laser ablation system (Photonic Instruments) focused through the epifluorescence optics of the Zeiss Axiovert 200M was used for photobleaching. After the capture of five pre-bleach baseline images at 5 s intervals, 515-nm laser pulses were directed at single dendritic spines for two repetitions at 75–85% maximum laser power to bleach YFP selectively. Directly after bleaching, 40 time-lapse images were captured at 5-s intervals. Pre-bleached intensities were averaged and set to 100%, and the immediate post-bleach image was set to 0%^{47,48}. The mobile fraction of calcineurin–YFP or AKAP79–YFP was estimated by fitting averaged recovery data to a single exponential curve.

- McCoy, A.J. *et al.* Phaser crystallographic software. *J. Appl. Crystallogr.* **40**, 658–674 (2007).
- Brünger, A.T. *et al.* Crystallography & NMR system: a new software system for macromolecular structure determination. *Acta Crystallogr. D Biol. Crystallogr.* **54**, 905–921 (1998).
- Wang, Z.X. An exact mathematical expression for describing competitive binding of two different ligands to a protein molecule. *FEBS Lett.* **360**, 111–114 (1995).
- Roehrl, M.H. *et al.* Selective inhibition of calcineurin–NFAT signaling by blocking protein–protein interaction with small organic molecules. *Proc. Natl. Acad. Sci. USA* **101**, 7554–7559 (2004).
- Gomez, L.L., Alam, S., Smith, K.E., Horne, E. & Dell'Acqua, M.L. Regulation of A-kinase anchoring protein 79/150–cAMP-dependent protein kinase postsynaptic targeting by NMDA receptor activation of calcineurin and remodeling of dendritic actin. *J. Neurosci.* **22**, 7027–7044 (2002).
- Robertson, H.R., Gibson, E.S., Benke, T.A. & Dell'Acqua, M.L. Regulation of postsynaptic structure and function by an A-kinase anchoring protein–membrane-associated guanylate kinase scaffolding complex. *J. Neurosci.* **29**, 7929–7943 (2009).
- Lippincott-Schwartz, J., Snapp, E. & Kenworthy, A. Studying protein dynamics in living cells. *Nat. Rev. Mol. Cell Biol.* **2**, 444–456 (2001).
- Sharma, K., Fong, D.K. & Craig, A.M. Postsynaptic protein mobility in dendritic spines: long-term regulation by synaptic NMDA receptor activation. *Mol. Cell. Neurosci.* **31**, 702–712 (2006).